Production and Characterization of Uniform and Graded Porous Polyamide Structures Using Selective Laser Sintering

M. Erdal[1], S. Dag[2], Y. A. C. Jande[3] and C. M. Tekin[4]
Department of Mechanical Engineering, Middle East Technical University, Ankara, Turkey
([1]merdal@metu.edu.tr, [2]sdag@metu.edu.tr, [3]e132160@metu.edu.tr, [4]e158635@metu.edu.tr)

Abstract - **In this study, uniform and graded porous polyamide structures are produced using selective laser sintering process by varying three processing parameters: hatching distance, laser power, and scanning speed. The PA 2200 polyamide powder is used to produce parts and the production is carried out in EOSINT P 380 laser sintering system. The effect of the three process parameters on porosity and mechanical properties are investigated on uniform porous structures using 2^3 factorial design. The produced samples are characterized in terms of apparent density, pore size distribution and microstructure. Tensile tests are carried out to assess the part mechanical properties with changing part porosities. Graded porous structures are then produced by varying the three process parameters during production, and characterized. It is concluded that a desired porosity grade within the limits of the machine capabilities can be induced in polyamide samples produced via SLS.**

Keywords - **Selective Laser Sintering, Porosity, Graded Structures, Factorial Design**

I. INTRODUCTION

Selective Laser Sintering (SLS) is a layered manufacturing technique that was developed originally to produce product models, usually with geometric complexity, in a rapid manner in order to speed up the prototyping stage of product design. In this process, product layers are formed by sintering a powder layer at select locations via a laser beam. Once a layer is sintered, a fresh layer of powder is laid on top of the sintered layer and the process repeats until the product is formed. Due to the discrete nature of manufacturing, all parts produced via SLS exhibit some porosity, the degree and the locality of which vary with respect to the process parameter settings, the SLS machine characteristics and the powder material. The ability to produce complex 3-D shaped parts in layered manufacturing offers a range of research opportunities in designing and developing porous materials that can find applications such as in thermal insulation and filtration. Furthermore, the porous structures can be infiltrated with a second material to produce composites [1] that have complex outer shapes, or graded materials, if the porosity can be varied within the part during production.

There have been prior studies on producing graded parts via SLS by utilizing more than one type of material [2-4]. Powder particle size has also been used as a means of imparting grades [5]. As a means of imparting varying degrees of porosity, laser power has been varied for the purpose of developing drug delivery devices [6].

In this study, uniform and graded mono-material porous structures are produced using selective laser sintering and characterized physically and mechanically. The amount of porosity is controlled by varying three processing parameters: the hatching distance (distance between two consecutive scan paths of the laser beam on a layer), the laser power and the laser scanning speed. The material used is the PA 2200 polyamide powder and the SLS system is the EOSINT P380 system. 2^3-factorial design is used to plan the production of uniformly porous structures and investigate the effect of the processing parameters on the resulting porous part properties

II. METHODOLOGY

By varying each of the three processing parameters between two levels, the 2^3-factorial design yields 8 production points. The default parameter setting of the SLS system (which the manufacturer recommends for producing models) is also added to the total number of production points. Table 1 presents these settings where HD stands for the hatching distance, LP, the laser power and SS, the scanning speed. In addition, the energy density (ED), which represents the combined effects of HD, LP, and SS, and defined as

$$ED = \frac{LP}{HD \times SS} \qquad (1)$$

is given in Table 1. The energy density (ED) roughly indicates the amount of energy to which a unit area of powder is exposed during production.

At each of the process settings given in Table 1, specimens have been produced for physical and mechanical characterization. The

produced parts are uniformly porous as the parameter setting during the production of each specimen remains fixed. Multiple characterization techniques have been employed therefore different sample geometries at each production setting were produced (Table 2). For part apparent density, which is indicative of porosity, and pore size distribution (using mercury porosimetry), cylindrical specimens have been produced. At each process setting, 4 repeat density specimens were produced in order consider possible production-related variability.

TABLE 1: PROCESSİNG PARAMETER SETTİNGS USED FOR THE 2^3-FACTORIAL DESIGN

No:	HD (mm)	LP (%)	SS (mm/s)	ED (J/mm^2)
1	0.45	66.3	5000	0.016
2	0.45	66.3	4000	0.019
3	0.45	90.0	5000	0.020
4	0.30	66.3	5000	0.024
5	0.45	90.0	4000	0.025
6	0.30	66.3	4000	0.029
7	0.30	90.0	5000	0.030
8*	0.30	90.0	4500	0.033
9	0.30	90.0	4000	0.037

* machine default setting

TABLE 2: SPECIMEN GEOMETRIES FOR PHYSICAL CHARACTERIZATION (DİMENSIONS IN mm)

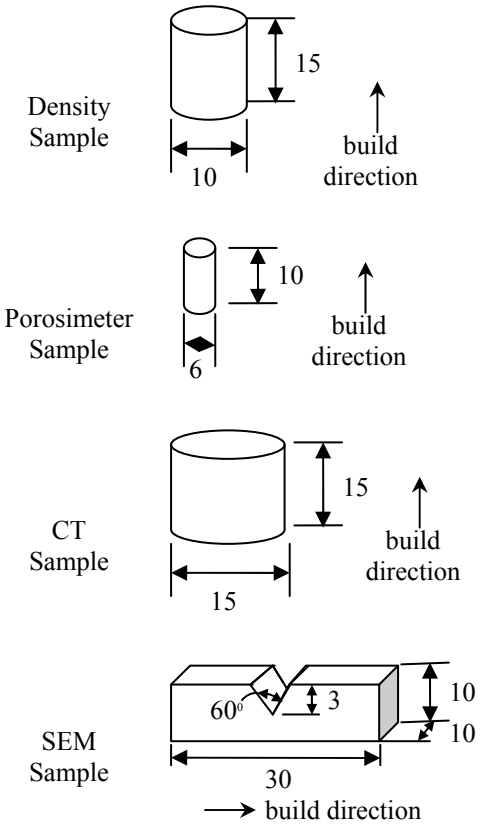

For visualizing the microstructure, scanning electron microscopy (SEM) was used. The samples for SEM are prismatic with a notch in the middle. In order to visualize as-processed inner layers, the SEM samples were cooled in liquid nitrogen and fractured at the notch plane. Computed tomography (CT) was used to determine the CT number at each process setting. The CT numbers were used later on as a reference in characterizing grades in graded specimens.

For mechanical characterization, dog-bone shaped specimens were produced at each process setting and tensile tests were carried out in accordance with ASTM Standard D 638-03 [7]. The ultimate tensile strength (UTS) of the produced samples is determined in these tests. At each setting, at least 4 repeat specimens were produced and tested, and the mean UTS value of those was taken as the specimen strength at that process setting. The sample geometry details are presented in Figure 1 and in Table 3.

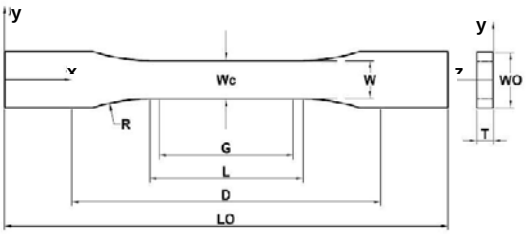

Build orientation
Layer plane: x-y plane
Build direction: z-axis

Figure 1: Sample for mechanical characterization and the layering direction

For graded specimens, grades have been implemented by changing the porosity in a specimen by varying the process settings during the production of a single specimen. The grades are given along the build direction; that is, the process setting on a layer does not change, however process settings change from one layer to another. The processing characteristics of the graded parts are given in Table 4. Each grade is expressed in terms of the energy density (ED), which denotes the process setting for that grade. The effects of number of grades have been studied by producing samples with 3-, 5- or 7-grades. Two different types of grade limits (maximum and minimum) have been set. In Type 1 parts, the minimum and maximum ED values are 0.016 J/mm^2 and 0.030 J/mm^2, respectively. In Type 2 parts, the minimum and maximum ED values are 0.019 J/mm^2 and 0.033 J/mm^2, respectively. The grade settings are chosen among the process settings used in producing uniformly porous structure (Table 1). The graded specimens are produced in the shape of mechanical test specimens (Figure 1).

TABLE 3: DIMENSIONS OF THE SPECIMEN SHOWN IN FIG. 1.

	Dimensions in mm
T – Thickness	6
W – Width of narrow section	13
W_c – Width at the center	13 (+0.00/-0.10)
L – Length of narrow section	57
WO – Overall width	19
LO – Overall length	165
G – Gage length	50
D – Distance between the grips	115
R – Radius of fillet	76

TABLE 4: THE GRADED POROUS PARTS PRODUCTION CONFIGURATION

		3-grades	5-grades	7-grades
ED (J/mm^2)	Type I	0.016	0.016	0.016
			0.020	0.019
		0.024		0.020
			0.025	0.024
		0.030	0.029	0.025
				0.029
			0.030	0.030
	Type II	0.019	0.019	0.019
			0.024	0.020
		0.025		0.024
			0.025	0.025
		0.033	0.030	0.029
				0.030
			0.033	0.033

Depending on the number of grades (3-, 5- or 7-grades), the grade thickness (i.e. the number of layers for each grade) changes so that the total part thickness in all graded specimens conforms to the ASTM Standard test specimen thickness (6 mm). Within a graded specimen, each grade has the same thickness. The samples are characterized in computed tomography, prior to the mechanical tests to determine the grade nature after production. In the SLS system used for production, the machine settings do not allow the variation of process settings within the production of a single solid model. Therefore, for the graded samples, each grade is modeled as a separate solid model and these solid models are stacked virtually on top of one another to form the intended product. For instance, the 3-grade Type 1 specimen is modeled as three dog-bone shaped solid models, each with a thickness of 2 mm (6 mm/3 grades), stacked on top of one another.

III. RESULTS AND DISCUSSION

Uniformly Porous Structures

A. Apparent Density

Apparent density (equation 2) is the mass of the specimen divided by its overall volume (including the pores). As such, it is indicative of specimen porosity; lower the apparent density is, higher the specimen porosity will be.

$$Apparent\ density = \frac{Specimen\ Mass}{Apparent\ Volume} \qquad (2)$$

The mass of the specimens are measured by weighing each in a digital triple beam balance. Since the specimens are cylindrical (Table 2), the overall volume is calculated from the measured diameter and height. Each dimension is measured at multiple locations on a part and the average value is taken as that dimension.

The apparent density of the specimens produced at the each of the process settings given in Table 1 are presented in Table 5. The density values are the mean values of the repeat specimens at each setting. The standard deviation is also given. The variation of the apparent density with energy density (ED) – the process setting indicator – is presented graphically in Figure 2.

TABLE 5: APPARENT DENSITY OF THE UNIFORMLY POROUS PARTS

ED (J/mm^2)	Apparent Density(g/cc)
0.016	0.7100±0.0150
0.019	0.7976±0.0196
0.020	0.8151±0.0211
0.024	0.9044±0.0013
0.025	0.9120±0.0088
0.029	0.9404±0.0067
0.030	0.9345±0.0044
0.033	0.9466±0.0039
0.037	0.9505±0.0112

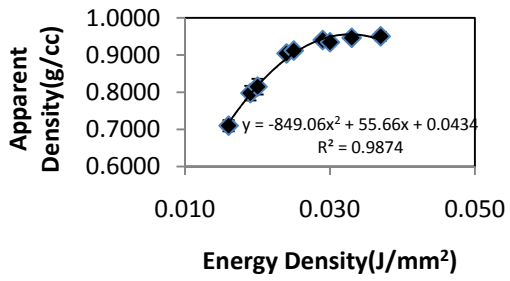

Figure 2: Variation of apparent density of the uniformly porous parts with energy density (ED)

The apparent density increases with increasing energy density (ED), as expected. Higher processing energy induces better fusion of the powder particles, leading to smaller porosity and larger apparent density. Beyond an ED value of 0.030 J/mm^2, the density does not show any significant change, reaching a value of about 0.95 g/cc. The significant variations occur at smaller ED values and with the process settings used, apparent density variation within the range 0.7 – 0.95 g/cc have been obtained. The standard deviations are small indicating small variability between productions, though the variability is higher at lower densities (higher porosities).

B. Ultimate Tensile Strength (UTS)

For the uniformly porous structures produced at the process settings of Table 1, the tensile tests are performed using a Zwick/Roell Z020 machine. The variation of part strength (UTS) with the process energy density (ED) is presented in Figure 3.

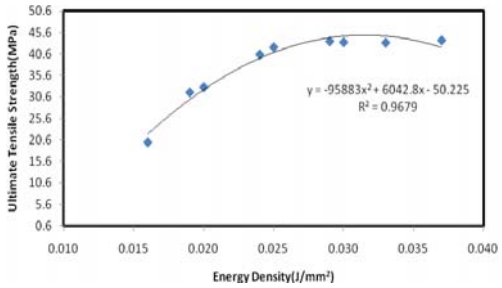

Figure 3: Variation of UTS with process energy density (ED)

As in the case of apparent density, the material strength increases with increasing process energy density (ED), reaching a nearly constant value beyond an ED value of 0.030 J/mm^2. Better fusion of powder particles yields stronger specimens. With the process settings used, the UTS varies within a range of approximately 20 – 44 MPa. Experiments have shown that further increasing the energy density does not yield higher material strength or lower porosity (higher apparent density) as the powder material begins degrading.

C. *Effects Analysis*

As the production of the uniformly porous specimens was designed using 2^3 - factorial design, the effect of each processing parameter on the obtained properties could be assessed. Figure 4 presents the individual and combined effects of the three processing parameters in the two resulting properties, apparent density and UTS. For each term (a single processing parameter or a term representing the combined effects of the processing parameters), the corresponding standardized effect on the response (the property of interest) is presented. The effects below the threshold value indicated by the straight vertical line in each graph are considered to be insignificant. It is seen that for the ranges of parameter levels used in the current production, the hatching distance alone has the major influence on the resulting porosity (apparent density) and the strength (UTS) of the sintered parts. This is followed by the laser power and the laser scanning speed, with some contribution from the combined effects. The combined effect of the three processing parameters and the combined effect of the laser power and scanning speed do not contribute to the resulting properties.

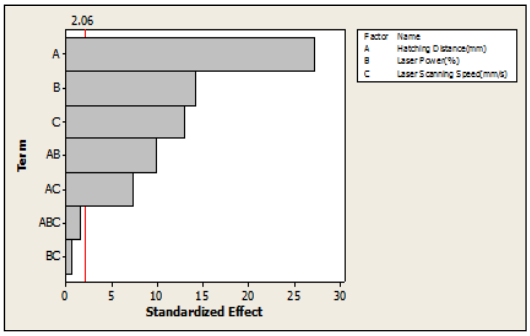

a) Standardized effects of individual and combined process parameters on uniformly porous specimen apparent density

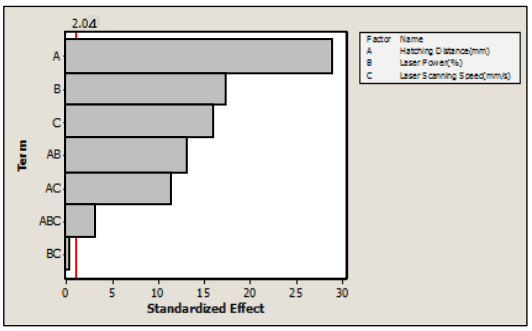

b) Standardized effects of individual and combined process parameters on uniformly porous specimen UTS

Figure 4: Effects of process parameters on uniformly porous part properties

If the process setting were to be changed in order to obtain a part with other density or strength values, a change in the hatching distance would yield the largest property change compared to changing the other process parameters in a similar amount. This information is also useful in optimizing the production; a regression model, fitting the effects, can be used to search for the process

setting that would yield a part with a desired porosity (density) with the maximum possible strength. However, these issues are out of the scope of this paper.

D. Microstructure

The microstructure of the uniformly porous specimens was examined qualitatively using SEM imagery (JEOL JSM electron microscope). Samples with ED values of 0.016 J/mm^2 (high porosity), 0.025 J/mm^2 (medium porosity) and 0.037 J/mm^2 (low porosity) were produced as specified in Table 2 and the fracture surfaces were scanned. Figures 5 and 6 show the SEM images of these samples.

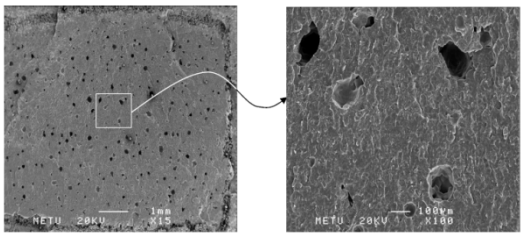

Figure 5: Microstructure of a low porosity sample (ED = 0.037J/mm^2)

The microstructure of the low porosity sample (produced at an energy density of 0.037 J/mm^2) is drastically different from the medium and low porosity samples. The particles are well fused forming an even layer with pores placed sparsely (Figure 5). The individual particles are indistinguishable. On the medium and the low porosity sample layer surfaces, particles are clearly distinguishable with the pores formed in between them (Figure 6). The powder particle size as reported by the manufacturer is, on the average, 60 μm. The images confirm this however, there are also smaller particles present and the individual powder particles also have some pores in them (Figure 6.b). The fracture surface for the low porosity sample is a single layer, whereas for the medium and low porosity samples, the fracture surface consists of several layers. As the process energy density gets smaller, the fusion between the layers gets weaker, the specimen fracturing along multiple numbers of layers.

E. Pore Size Distribution

The pore size distributions in uniformly porous samples were determined using mercury porosimetry (Quantachrome Corporation, Poremaster 60). Three production settings were analyzed (ED = 0.016, 0.025, and 0.037 J/mm^2). The samples shown in Table 2, were impregnated with mercury at progressively increasing pressure. The pore size through which mercury can infiltrate at a given pressure is known. Tracking the amount of mercury infiltrated at each pressure and using the pressure-pore size correlation, the pore size distributions were obtained. The results are presented in Figure 7.

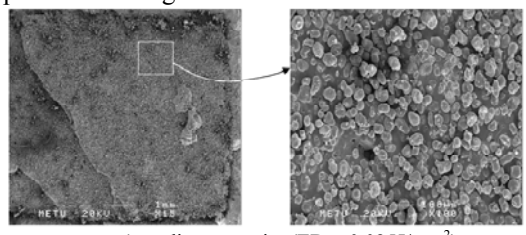

a) medium porosity (ED = 0.025J/mm^2)

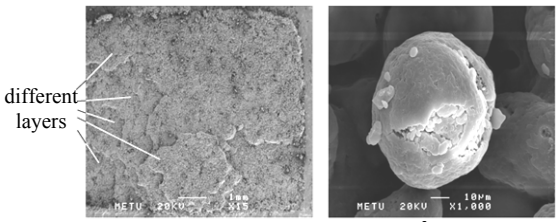

b) low porosity (ED = 0.016J/mm^2)

Figure 6: Microstructure of medium and high porosity samples

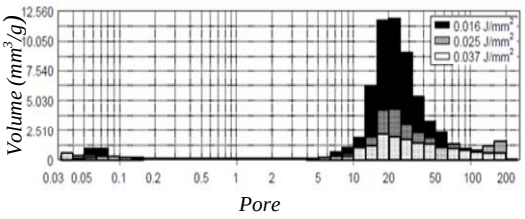

Figure 7: Pore size distribution in uniformly porous specimens produced at ED = 0.016 J/mm^2 (high porosity), 0.025 J/mm^2 (medium porosity) and 0.037 J/mm^2 (low porosity)

As expected, the largest volume of pores is in the high porosity part (lowest ED), with the overall pore volume decreasing as the energy density, ED, increases and porosity decreases. The size distribution in all cases is in the shape of a bell curve, with the majority of the pores in the size range of 5-100 μm. Thus, the formed pores are macropores and the largest volume of pores occurs at the pore size of around 20 μm in all process settings. It could be argued that different production settings which yield significantly different microstructures observed in Figure 5 and 6, would yield the largest concentration of pore volume at different pore sizes. However, Figure 7 clearly shows this is not the case, implying that the powder particle size, which is the fixed effective parameter in all settings, is the major influence on the size of the largest volume of pores.

Graded Porous Structures

A. Computed Tomography (CT) Results

Uniformly porous samples, cylindrical in shape given in Table 2, were produced at the process settings of Table 1 to construct a reference scale relating the process energy density (ED) to the CT number obtained by computed tomography. Since the CT number will relate to a specific energy density (ED) (through the constructed reference scale), obtaining the CT number variation within a graded specimen will allow the characterization of its inner structure.

In order to construct the CT number vs. ED scale, three layers on the uniformly porous specimens are scanned in CT and the average CT number of the three layers is taken as the CT number corresponding to the ED value of that specimen (Figure 8). Figure 9 presents the constructed reference scale. It is seen that the CT number correlates in a very similar manner as the apparent density of Figure 2. This is expected as the CT value relates directly to porosity. The standard deviations at each value are small. Thus, the variations in microstructure from one layer to another are small and uniformly porous structures could indeed be produced by SLS.

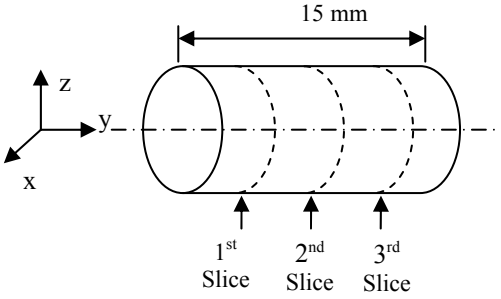

Figure 8: Scanned layers in uniformly porous specimens in computed tomography

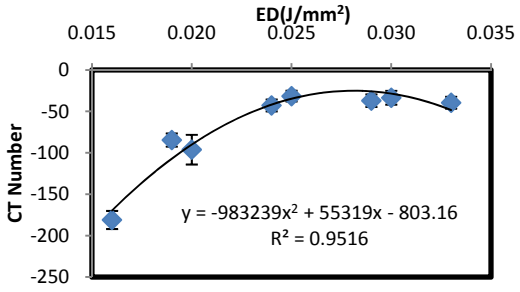

Figure 9: Variation of CT-number with energy density (ED)

The graded samples were produced in the dog-bone shape of Figure 1 with respect to the settings of Table 4. The grade direction was along the thickness and the specimens were scanned on layers normal to the thickness direction in computed tomography. On each layer, several points along the width direction (y-direction of Figure 1) were scanned and the average of those was taken as the mean CT value at that thickness level. Using the scale of Figure 9, the expected CT values for each grade could be constructed. The expected and the measured CT values are presented in Figures 10 and 11.

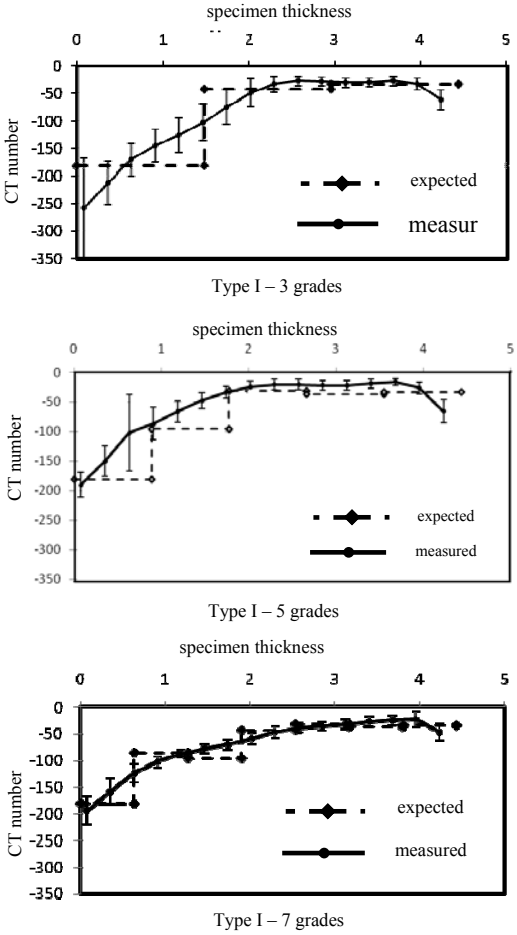

Figure 10: Comparison of expected and measured grade trends for Type I graded specimens

In all graded specimens, the grade changes occur in a continuous, smooth manner, rather than in step changes as which the process settings were entered into the SLS system. The Type II specimens show significant deviation from expected trends, yielding almost a homogenous CT distribution with little grading, except at the two edges of the parts. The standard deviations of these CT values are also significantly high. On the other hand, the Type I specimens exhibit clear, continuous grades with close match with the expected trends. As the number of grades increase, the measured trends conform more to the expected trends.

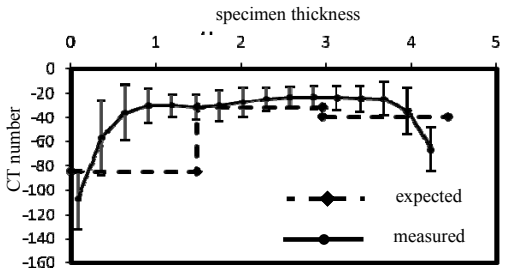

Type II – 3 grades

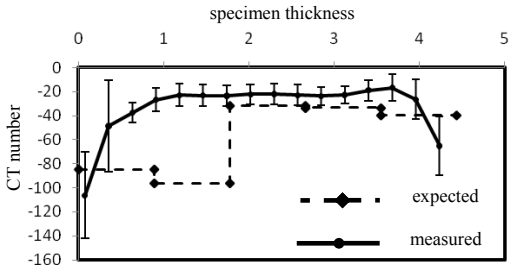

Type II – 5 grades

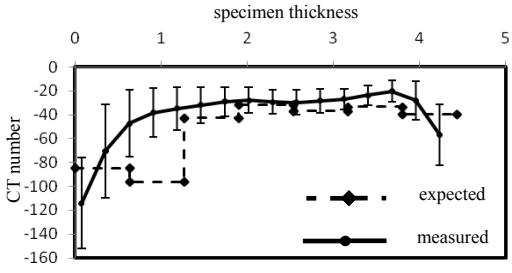

Type II – 7 grades

Figure 11: Comparison of expected and measured grade trends for Type II graded specimens

B. Ultimate Tensile Strength (UTS) and Rupture Strength

The graded specimens were next tested in the tensile testing system (Zwick/Roell Z020) and the obtained ultimate tensile strength (UTS) and rupture strength values are presented in Figure 12. The overall strength of a graded product does not signify a crucial property as it does in homogenous structures however it can contribute the understanding of the influence of different grades on the product.

It is seen that the UTS and rupture strength of the specimens are very close to one another, with the only exception in Type I – 7 grade specimen. In each type, the strength values are not significantly affected from the number of layers. For Type I specimens, the UTS values vary between 34.97 and 35.72MPa, and the rupture strength between 33.39 and 35.30MPa – quite a small variation. For Type II specimens, the UTS values vary between 39.89 and 40.69MPa, and the rupture strength between 39.72 and 40.58MPa, again very small variations. In Type II specimens, the CT measurements had shown very small grading, with the majority of the specimens resembling homogenous parts built at the energy density of 0.25 – 0.33 J/mm^2. In this ED range, the uniformly porous structures had exhibited strength values around 40 – 44 MPa (Figure 3). The Type II specimen strength values conform to those results. In Type I specimens, the grades could clearly be distinguished in the CT results. The strength values, though not as high as that corresponding to the largest ED setting (0.30 J/mm^2) - about 43 MPa (Figure 3), still exhibit a significantly high value around 35 MPa. For the production ED range used in Type I specimens, the individual grade strengths would vary between 20 – 43 MPa per results of Figure 3. As such, the Type II graded specimens were not as strong as their weakest grade, but actually stronger, approaching a mid-strength value in the produced grade spectrum.

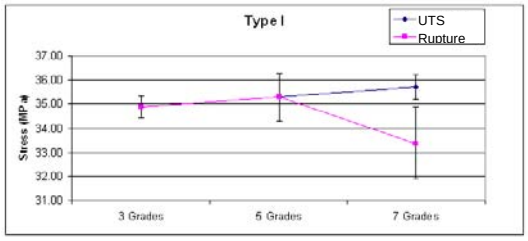

(a) UTS and rupture strength of Type I graded specimens

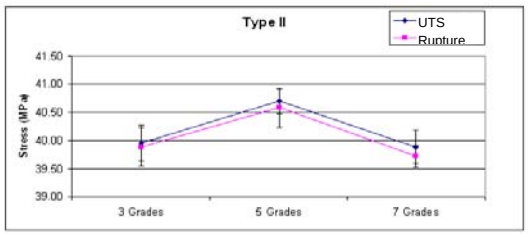

(b) UTS and rupture strength of Type II graded specimens

Figure 12: UTS and rupture strength of graded specimens

IV. CONCLUSIONS

In this study, uniform and graded porous polyamide structures were produced on the EOSINT P380 selective laser sintering system, using PA 2200 polyamide powder. The porosity was varied by controlling the three processing parameters: hatching distance, laser power, and scanning speed. Within the production parameter range used, porous samples with apparent densities ranging from 0.7 g/cc to 0.95 g/cc could be produced in a controlled, repeatable manner. The majority of the pores in all specimens were found to have a pore size around 20 μm, regardless of the production

setting or the overall porosity. The produced porous samples exhibited strength values in the range 20 – 45 MPa. An effects analysis based on 2^3 factorial design showed that hatching distance was the most influential process parameter within the parameter ranges used in production. Graded porous structures were produced by controlling porosity through varying the process settings within each specimen. With the proper process setting range, a clear, continuous grade could be obtained (Type II specimens), close to the designed grade profile. The number of grades did not affect the overall strength, however, the maximum/ minimum porosity limits did. The graded specimens were found to be stronger than their weakest grade. It is concluded that a desired porosity grade within the limits of the machine capabilities could be induced in polyamide samples produced via SLS.

ACKNOWLEDGMENT

This work is supported by the Scientific and Technical Research Council of Turkey (TUBITAK) through grant 106M437.

REFERENCES

[1] Erdal, M., Ertoz, L. and Güçeri, S., "Characterization of permeability for solid freeform fabricated porous structures". *Proc. The Science, Automation and Control of Material Processes Involving Coupled Transport and Rheology Changes*, MD-Vol.89, 1999, pp. 57-63.

[2] K. A. Mumtaz and N. Hopkinson, "Laser melting functionally graded composition of Waspaloy® ", *Material Science* 42, 2007, pp.7647–7656

[3] H. Chung and S. Das, "Functionally graded Nylon-11/silica nanocomposites produced by selective laser sintering ", *Material Science and Engineering* A 487, 2007, pp.251–257.

[4] H. Chung and S. Das, "Processing and properties of glass bead particulate-filled functionally graded Nylon-11 composites produced by selective laser sintering ," *Materials Science and Engineering* A 437, 2006, pp.226–234.

[5] G. V. Salmoria, C. H. Ahrens, P. Klauss, R. A. Paggi, R. G. Oliveira, A. Lago, "Rapid manufacturing of polyethylene parts with controlled pore size gradients using selective laser sintering", *Material Research*, vol.10, no.2, pp.1-9, 2007.

[6] K. F. Leong, C. K. Chua, W. S. Gui, "Building porous biopolymeric microstructures for controlled drug delivery devices using selective laser sintering ", *Advanced Material Technology,* vol.31, pp. 483–489, 2006.

[7] S. Bose, J. Darsell, H. L. Hosick, L. Yang, D. Sarkar, A. Bandyopadhyay, "Processing and characterization of porous alumina scaffolds ", *Material Science,* vol.23,no.1, pp. 23-28, 2002.